Supporting Information

Ionothermal synthesis of a photoelectroactive titanophosphite with three-dimensional open-framework

Junbiao Wu,[a] Luqi Lou,[a] Hang Liu,[b,c] Tan Su,[d] Zhuopeng Wang*[a] and Jiyang Li*[b]

a. Department of Chemistry, College of Science, Northeastern University, Shenyang, Liaoning 110819, P. R. China. E-mail: wangzhuopeng@mail.neu.edu.cn; Fax: (+86) 024 8368-4533; Tel: (+86) 024 8368-4533

b. State Key Laboratory of Inorganic Synthesis and Preparative Chemistry, College of Chemistry, Jilin University, Changchun 130012, P. R. China. E-mail: lijiyang@jlu.edu.cn; Tel: (+86) 431 8516-8608; Fax: (+86) 431 8516-8608.

c. Everdisplay Optronics Limited, Shanghai 201506, P. R. China.

d. Laboratory of Theoretical and Computational Chemistry, Institute of Theoretical Chemistry, Jilin University, Changchun 130021, P. R. China

1. Synthesis of JIS-15

The reagents and solvents employed were commercially available and used as received without further purification. In the typical synthesis of JIS-15, the mixture of titanium power (0.24 g, 5 mmol), H_3PO_3 (0.42 g, 50 mmol), HF (0.1 mL, 40%wt, 2.25 mmol), and the ionic liqiud of [EMIM] [Br] (1.0 g, 5.3 mmol) heated at 170°C for 7 days in a Teflon-lined stainless steel autoclave under static conditions in an oven. The resulting colorless single crystals of JIS-15 were collected and washed with deionized water, and dried at 353 K, the product yield is 67% based on Ti. JIS-15 can also be obtained by means of titanium isopropoxide (1.5ml, 5mmol, 98%) and tetrabutyl titanate (1.7ml, 5mmol, 99%) as the titanium sources, the product yields are 56% and 62% based on Ti, respectively. Compositional Anal. Calc. (%) for $TiP_2O_6H_2$ (207.83): Ti 23.03, P 29.81, H 0.97; found (%): Ti 23.86, P 30.32, H 1.03.

2. Experimental characterization

Inductively coupled plasma (ICP) analysis was performed on a Perkin-Elmer Optima 3300DV spectrometer. Elemental analysis was conducted on a Perkin-Elmer 2400 elemental analyzer. Powder X-ray diffraction (XRD) and *in-situ* temperature dependent X-ray diffraction data were both collected on a Rigaku D-Max 2550 diffractometer with Cu Kα radiation (λ = 1.5418 Å). The *in-situ* temperature dependent X-ray diffraction of JIS-15 were performed at a heating rate of 10 $^oC\ min^{-1}$, and the data were collected at a rate of 6° min^{-1}. Infrared (IR) spectrometry was performed with a Nicolet Impact 410 FTIR infrared instrument. Scanning electron microscope (SEM) images of crystal morphology were recorded on a JSM 6510 microscope at an acceleration voltage of 20 kV. X-ray photoelectron spectroscopy (XPS) measurements were performed using a Thermo Escalab 250 spectrometer with monochromatized Al Kα excitation. The UV/Vis absorption spectra were recorded at room temperature on a shimadzu UV-2450 spectrophotometer. UV-Vis-NIR spectrum of JIS-15 was performed on a Lambda 750s spectrophotometer. The surface photovoltage (SPV) measurement system was composed of a monochromatic light source, a lock-in amplifier (SR830-DSP) with a light chopper (SR540), a sample cell, and a computer. A 500-W xenon lamp and a double-prism monochromator provided the monochromatic light. In the

photovoltaic cell, the powder sheet was directly sandwiched between two blank indium tin oxide (ITO) electrodes. The field-induced surface photovoltage spectroscopy (FISPS) is a supplement to the SPV spectroscopy method. In FISPS, the external electric fields were applied between the two electrodes. The photocurrent experiments were performed on a CHI660E electrochemistry workstation in a three electrode system, with the sample-coated ITO glass as the working electrode mounted on the window with an area of 1.0 cm^2, a Pt wire as auxiliary electrode, and a saturated calomel electrode (SCE) as reference electrode. The supporting electrolyte solution was a 0.2 mol· L^{-1} sodium sulfate aqueous solution. The applied potential was 1 V for all measurements. The lamp (300W,1.35W/cm^2) was kept on continuously, and a manual shutter was used to block exposure of the sample to the light. The sample was typically irradiated at intervals of 20 seconds. Mott-Schottky (MS) measurements were performed in 0.5 mol/L Na_2SO_4 solution using an electrochemical workstation (CHI660E, China) with a three-electrode system at room temperature.

3. Single-crystal X-ray diffraction

Suitable single crystal with dimensions of 0.22 × 0.21 × 0.18 mm^3 for JIS-15 was selected for single-crystal X-ray diffraction analysis. The intensity data were collected on a Bruker SMART APEX Ⅱ CCD diffractometer by oscillation scans using graphite-monochromated Mo Kα radiation (λ = 0.71073 Å) at temperature of 23±2°C. Cell refinement and data reduction were accomplished with the SAINT processing program. The structure was solved in monoclinic space group $P2_1/n$ (No. 14) by direct methods and refined by full matrix least-squares technique with the SHELXTL-2014 crystallographic software package. (*G.M. Sheldrick. Acta Cryst. (2015). C71, 3-8*) All framework atoms Ti, P and O could be unambiguously located. All non-hydrogen atoms were refined anisotropically. The coordinates of the unique hydrogen atom H1 bonded to P1 were refined isotropically yielding P1-H1 1.323(3) Å. CCDC 1019743 contains the supplementary crystallographic data for this paper. These data can be obtained free of charge from The Cambridge Crystallographic Data Centre via www.ccdc.cam.ac.uk/data_request/cif.

4. Evaluation of photocatalytic activity

Photocatalytic activity experiments were performed under a 300 W xenon lamp source (PLS-SEX300/300 UV type, CEAULIGHT Beijing) with a 420 nm cut-off filter (420 nm< λ < 760 nm). The photocatalytic degradation experiment was as following: The photocatalyst of 50 mg was dispersed in 100 mL RhB solution (5 mg L^{-1}) under the constant stirring. Prior to illumination, the mixture was placed in the dark and magnetically stirred for 30 min to make the adsorption desorption equilibrium between RhB solution and photocatalyst. Then, the mixture was irradiated in a quartz reactor under continuous stirring. 3 mL of the clear solution was removed at certain time intervals during the irradiation, and the concentration of RhB solution in the reactor was determined by a UV−vis spectrophotometer at 554 nm.

The degradation efficiency of RhB dyes was analyzed by the following equation:

Degradation efficiency (%)= $(C_0 - C)/ C_0 \times 100$

Table S1. Crystal data and structure refinement for JIS-15 [a]

Empirical formula	$H_2O_6P_2Ti$
Formula weight	207.86
Temperature	296(2) K
Wavelength(Å)	0.71073
Crystal system, space group	Monoclinic, $P2_1/n$
Unit cell dimensions	
a (Å)	4.8518(3)
b (Å)	8.1747(5)
c (Å)	6.8142(4)
α(deg)	90
β(deg)	105.4680(10)
γ (deg)	90
Volume(Å^3)	260.48(3)
Z, calculated density(mg m^{-3})	2, 2.650
Absorption coefficient(mm^{-1})	2.208
F(000)	204
Crystal size(mm^3)	0.220 × 0.210 × 0.180
θ range(°) for data collection	3.98–28.22
Limiting indices	$-2 \le h \le 6$, $-10 \le k \le 10$, $-8 \le l \le 9$
Reflections collected/unique	1833/643, [R(int) = 0.0179]
Completeness to θ (%)	25.24, 100
Absorption correction	semi-empirical from equivalents
Refinement method	full-matrix least-squares on F^2
Data/restraints/parameters	643 / 0 / 47
Goodness-of-fit on F^2	1.160
Final R indices [$I > 2\sigma(I)$]	R_1 = 0.0232, wR_2 = 0.0672
R indices (all data)	R_1 = 0.0249, wR_2 = 0.0681
Largest diff. peak and hole (e Å^{-3})	0.290 and -0.440

[a] $R_1 = \sum(\Delta F/\sum(F_o))$, $wR_2 = (\sum[w(F_o^2 - F_c^2)])/\sum[w(F_o^2)^2]^{1/2}$ and $w = 1/\sigma^2(F_o^2)$.

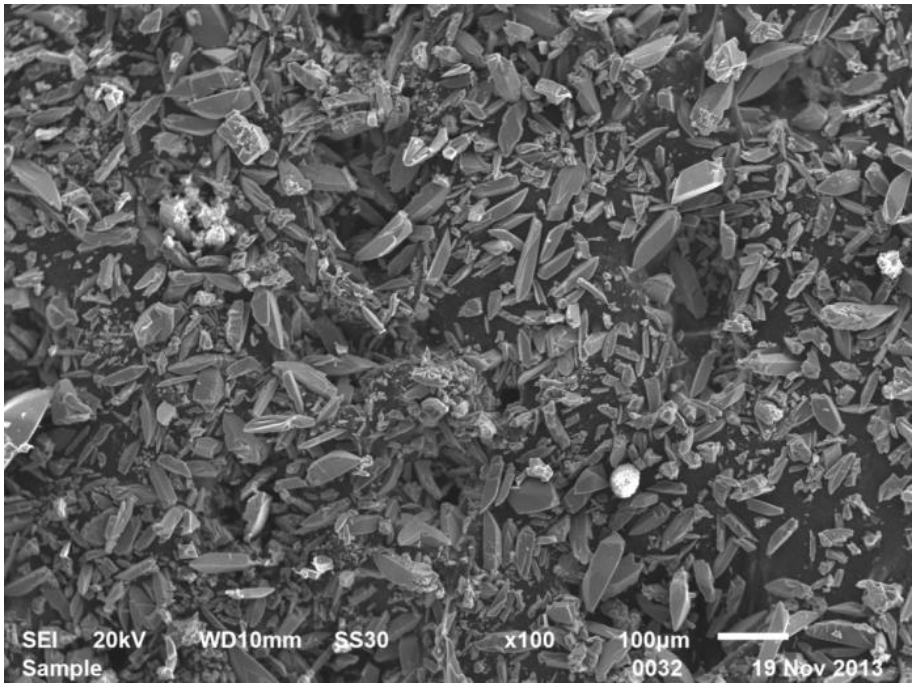

Figure S1 SEM image of JIS-15 using titanium power as titanium source, which shows shuttle-like crystals smaller than 100 μm.

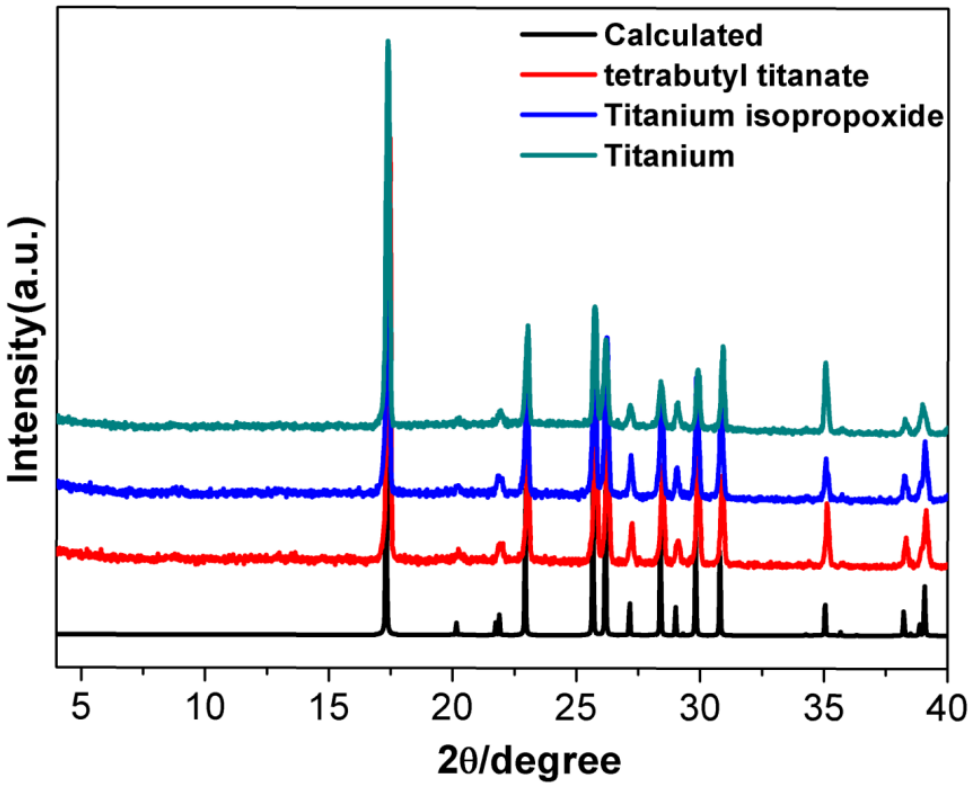

Figure S2 Experimental and simulated powder XRD patterns for JIS-15 synthesized by different titanium sources: titanium power (olive line), titanium isopropoxide (blue line), tetrabutyl titanate (red line), indicating the good phase purity.

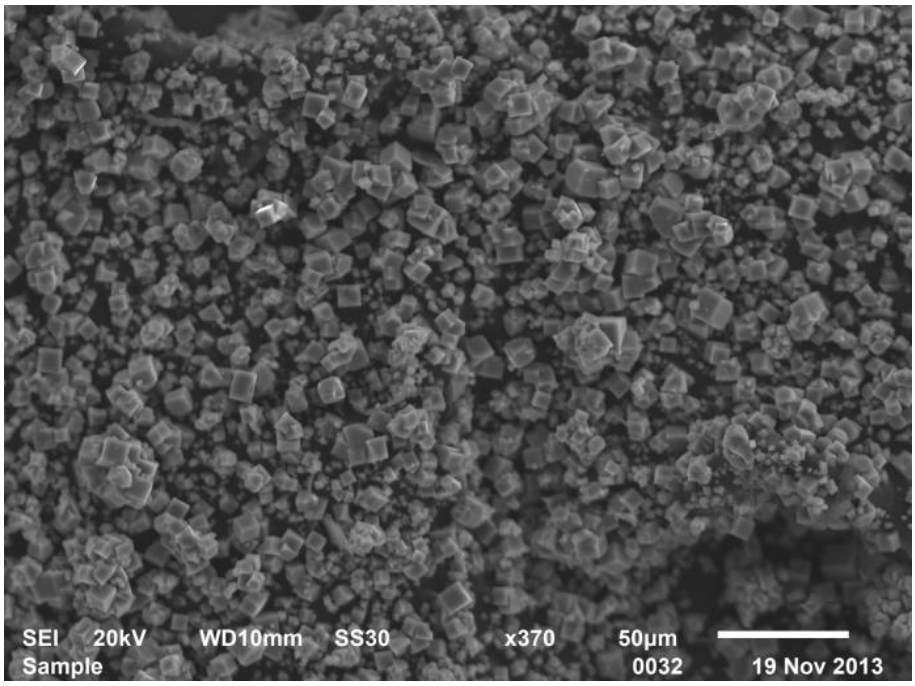

Figure S3 SEM image illustrates the product obtained from the same synthesis system as JIS-15 except for the absence of F^- ions. The cubic crystals are $Ti_2P_2O_7$.

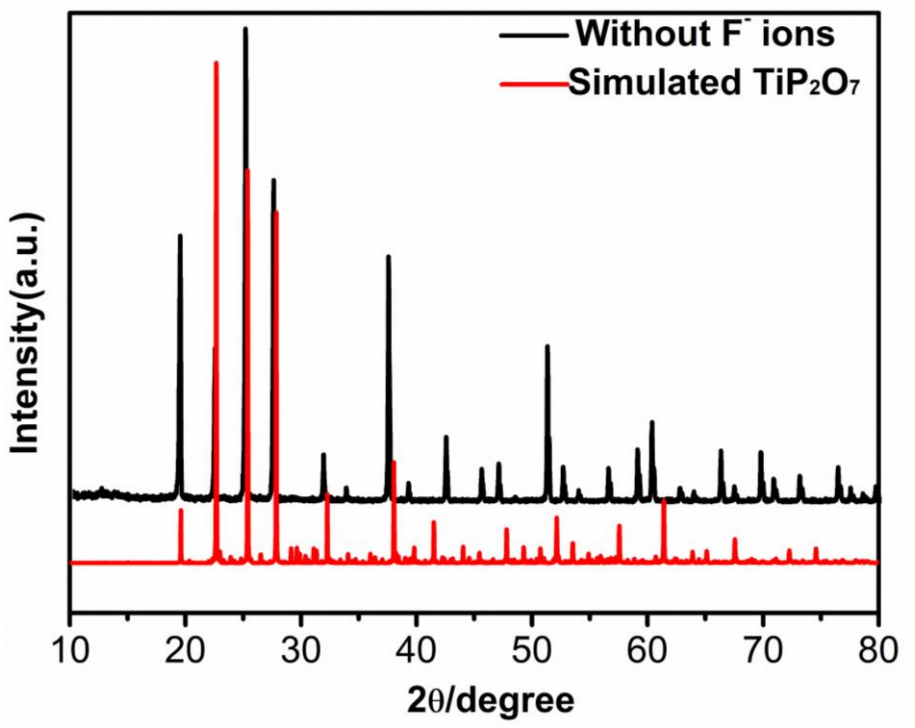

Figure S4 Experimental and simulated powder XRD patterns for $Ti_2P_2O_7$ obtained in the absence of F^- ions.

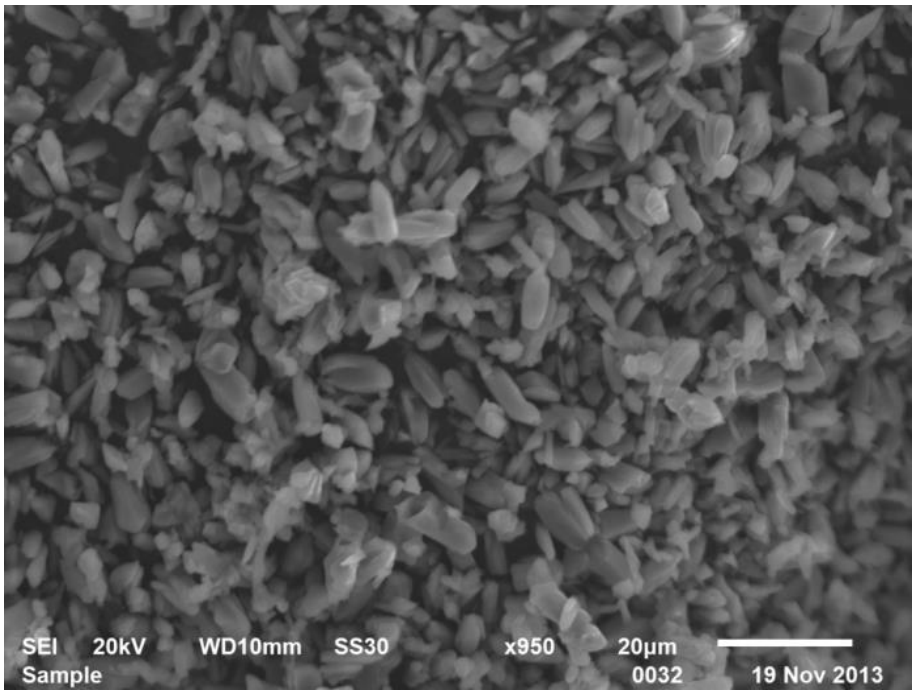

Figure S5 SEM image of JIS-15 using tetrabutyl titanate as titanium source, which shows shuttle-like crystals smaller than 10 µm.

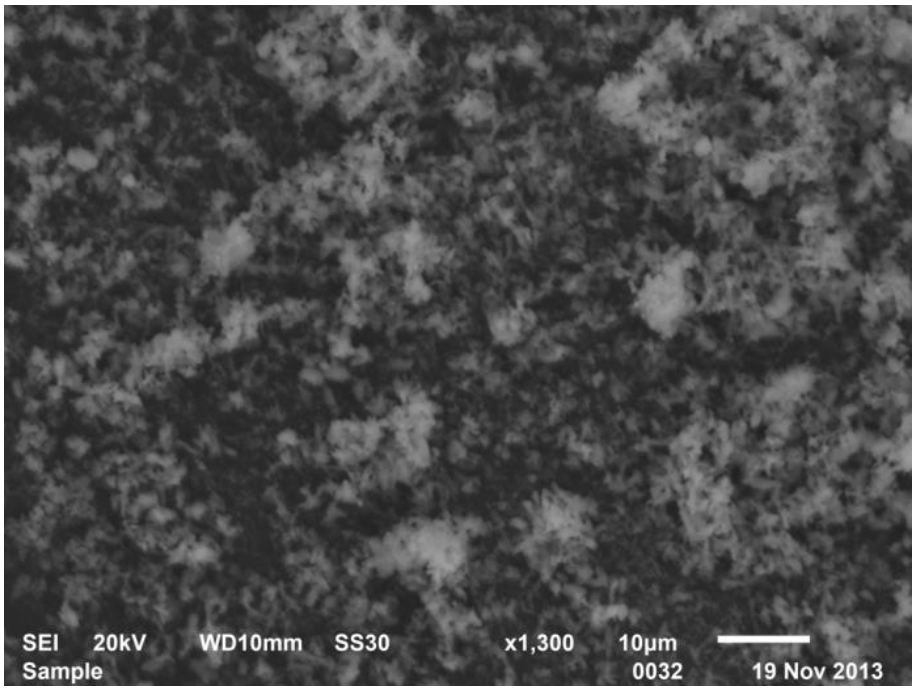

Figure S6 SEM image of JIS-15 using titanium isopropoxide as titanium source, which shows needle-like crystals smaller than 5 µm.

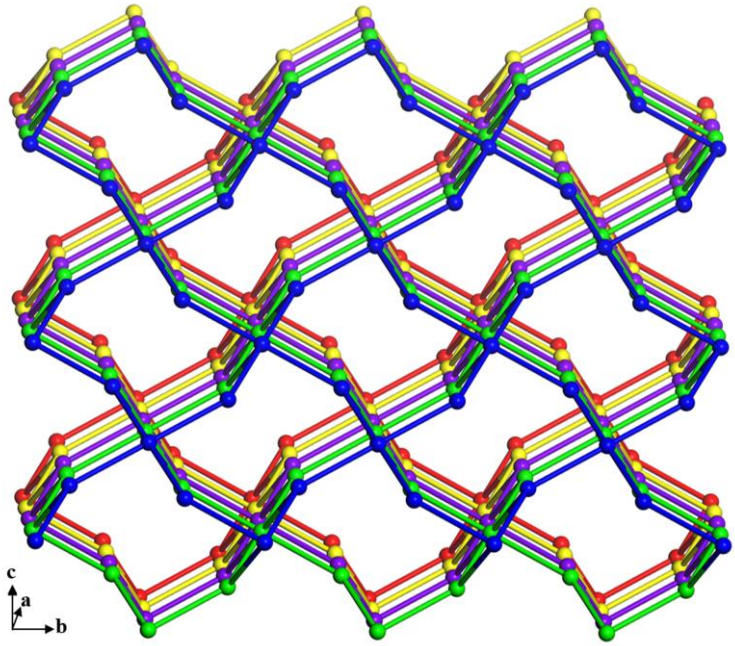

Figure S7 Structure of JIS-15 with distorted 8-ring channels along the [100] direction. (H and O atoms are omitted for clarity)

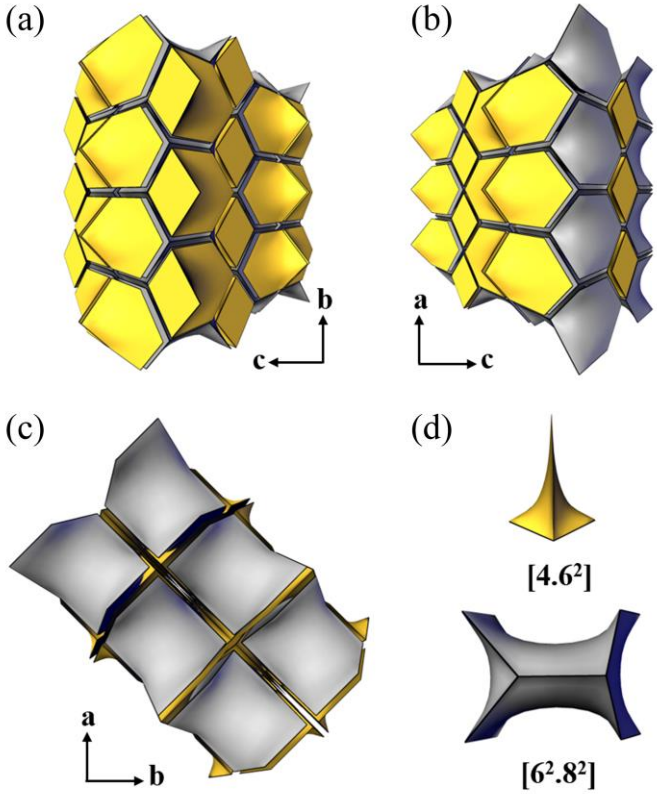

Figure S8 Natural tiling of JIS-15 with signature of $[4.6^2]$ + $[6^2.8^2]$ runs along the *bc* plane, *ac* plane and a*b* plane.

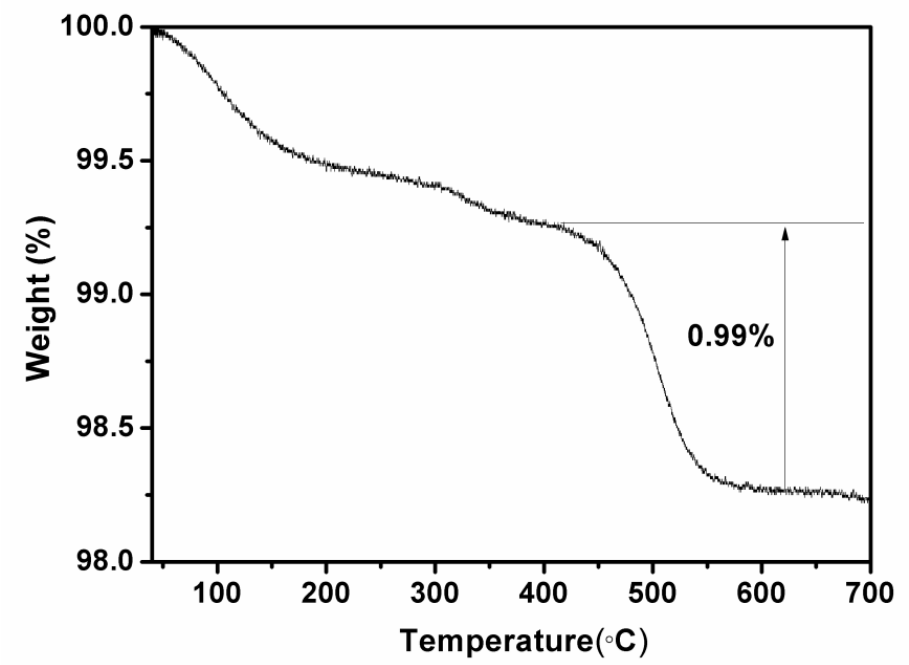

Figure S9 TG curve of JIS-15, shows a weight loss of 0.99 wt% from 400 °C to 700°C, corresponding to the loss of hydrogen (calc. 0.97 wt%).

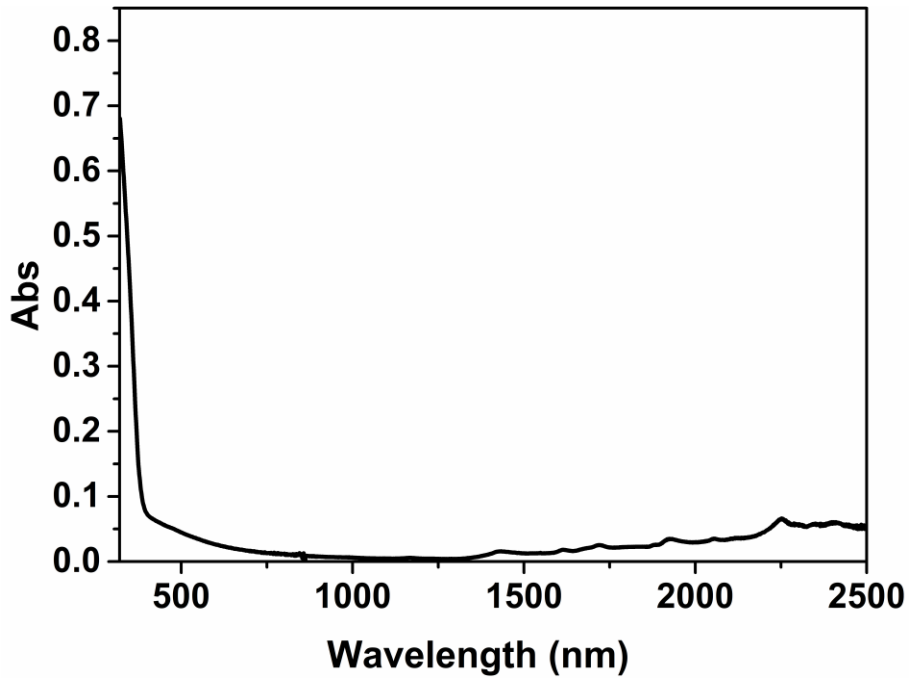

Figure S10 UV-Vis-NIR spectrum of JIS-15, which shows almost no absorption of infrared light.

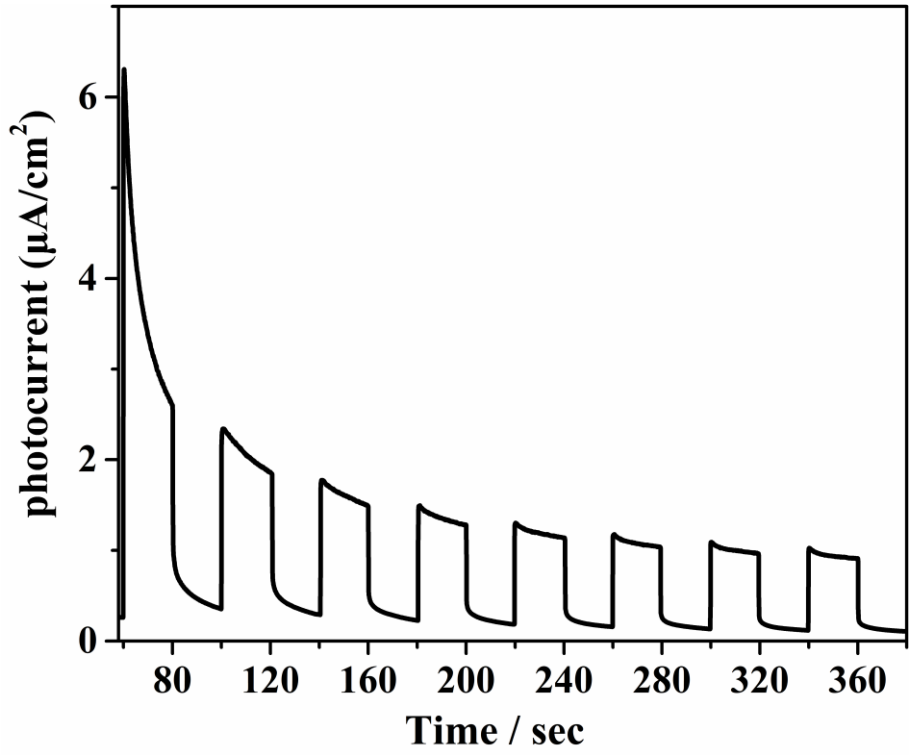

Figure S11 Transient photocurrent density of JIS-15, indicating the effective separation of the photogenerated electron–hole pairs under visible-light irradiation.

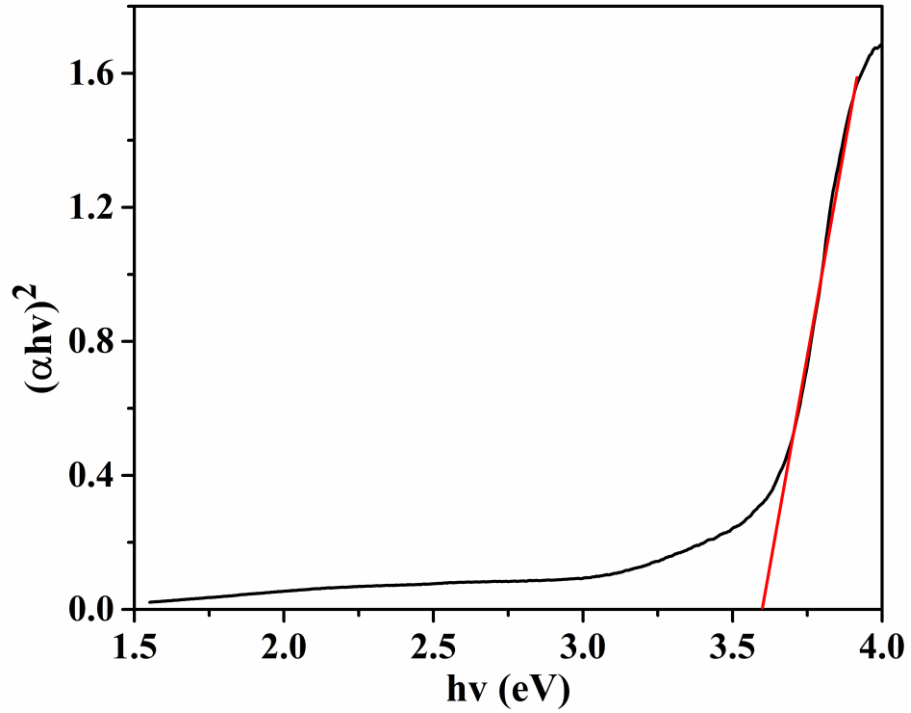

Figure S12 Plot of $(\alpha hv)^2$ as a function of hv for the bandgap energy of JIS-15, exhibiting its bandgap energy estimated to be 3.59 eV.

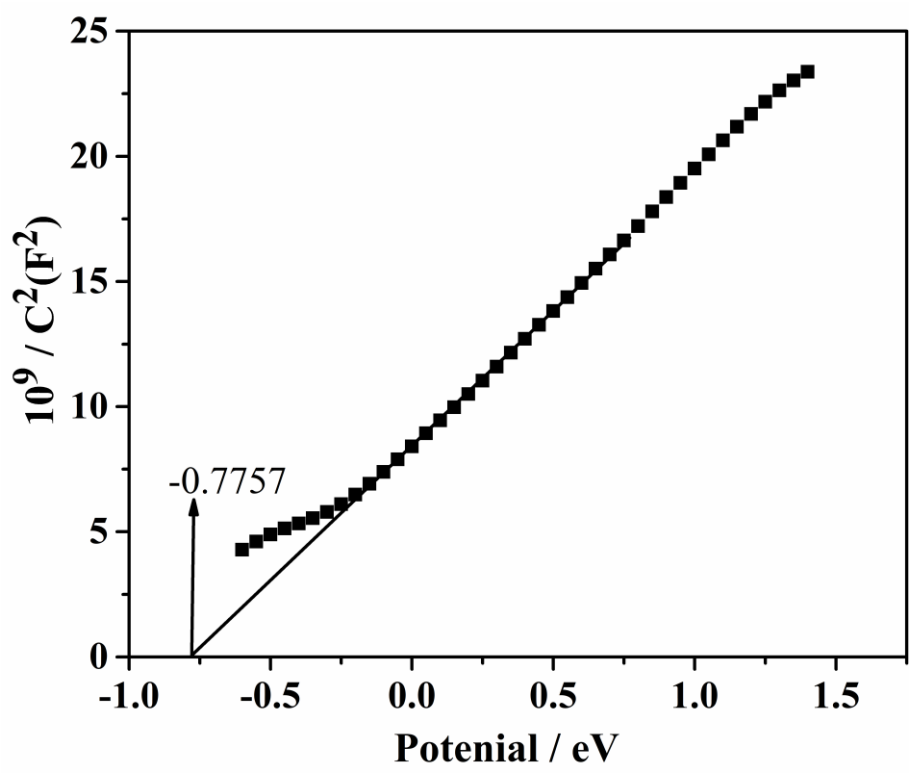

Figure S13 Mott-Schottky plot of JIS-15, the positive slope indicates an n-type semiconductor.

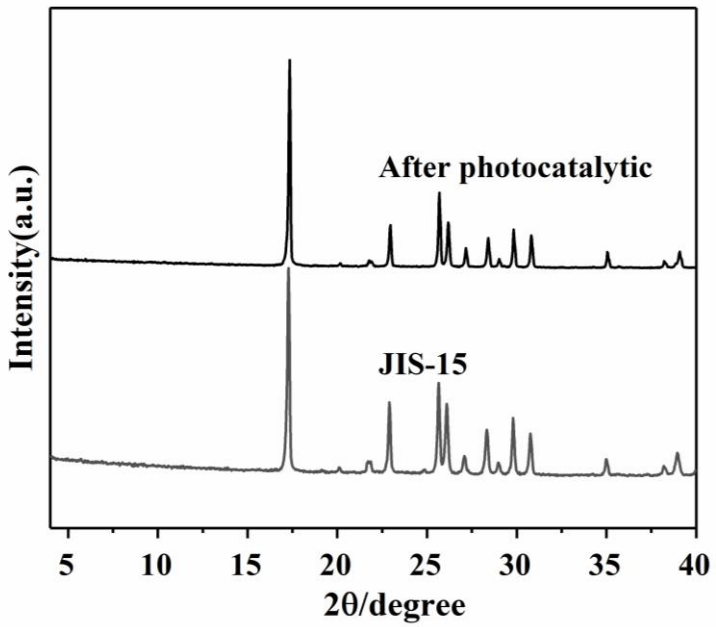

Figure S14 Powder XRD patterns of JIS-15 before and after photocatalytic reaction, exhibiting the stability of photocatalyst.

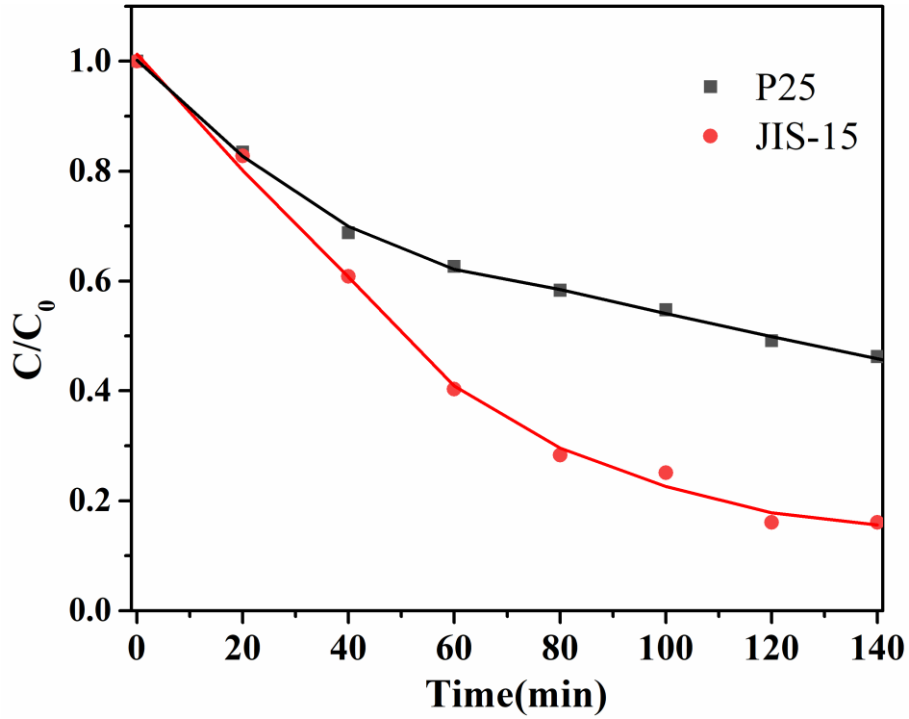

Figure S15 Photocatalytic degradation of RhB of JIS-15 and P25 under visible-light irradiation at the same conditions.